Self-organized 40 Hz synchronization in a physiological theory of EEG

I. Bojak *,[1] and D.T.J. Liley

Centre for Intelligent Systems and Complex Processes, LSS H31, Swinburne University of Technology, PO Box 218, Hawthorn, VIC 3122, Australia

Abstract

We present evidence that large-scale spatial coherence of 40 Hz oscillations can emerge dynamically in a cortical mean field theory. The simulated synchronization time scale is about 150 ms, which compares well with experimental data on large-scale integration during cognitive tasks. The same model has previously provided consistent descriptions of the human EEG at rest, with tranquilizers, under anaesthesia, and during anaesthetic-induced epileptic seizures. The emergence of coherent gamma band activity is brought about by changing just one physiological parameter until cortex becomes marginally unstable for a small range of wavelengths. This suggests for future study a model of dynamic computation at the edge of cortical stability.

Key words: Electroencephalogram; Self-organization; Gamma band; 40 Hz; Synchronization

1. Introduction

Observed scalp EEG activity is generated by masses of excitatory neurons firing in local synchrony. Most of the this rhythmic activity occurs at low frequencies: typically $> 90\%$ of the power spectrum resides below 20 Hz in an awake and restful state. There is however experimental evidence that cognitive tasks lead to oscillatory synchronization at large scales (> 1 cm) in the brain, which occur with appropriate conduction delays of $\gtrsim 100$ ms. Typically such synchronization is seen in the gamma band (around 40 Hz), see for example Refs. [1–5] and references therein. One can speculate that such activity signals the coordination of spatially distributed assemblies of neurons engaged in a common task. One can further speculate that precise temporal correlation of such assemblies of neurons 'binds' together their dynamic functions [6–8].

Bojak and Liley [9] have shown that a mean field theory can reproduce the typical frequency spectrum and firing rates of the human EEG, and at the same time can predict the effects of general anaesthetic agents (GAs) on the EEG. It is of particular interest here that the model can explain the counter-intuitively proconvulsant properties of many volatile GAs as a Hopf bifurcation occurring during the increase of GA concentration, which initiates an epileptic seizure [10]. Epileptic seizures are well known for their large scale coherence, albeit at low frequencies. So it is natural to ask whether the model also supports large scale coherence at gamma band frequencies, a feature central to some explanations of cognition [6–8].

Our model [9] has been found to generate a rich range of dynamics in spite of being constrained to physiologically plausible parameterizations. It describes the mean field dynamics of large populations of cortical neurons through a set of two-dimensional nonlinear partial differential equations (PDEs). EEG voltage is then linearly related to h_e, the mean excitatory soma membrane potential [11]. With $k, l = e(\text{xcitatory}), i(\text{nhibitory})$ the PDEs are

* Corresponding author: ibojak@swin.edu.au.

[1] Supported by grant DP0559949 from the ARC.

$$\tau_k \frac{\partial h_k(\boldsymbol{x}, t+\xi)}{\partial t} = -\left[h_k(\boldsymbol{x}, t+\xi) - h_k^{\mathrm{r}}\right] + \sum_l \frac{h_{lk}^{\mathrm{eq}} - h_k(\boldsymbol{x}, t+\xi)}{|h_{lk}^{\mathrm{eq}} - h_k^{\mathrm{r}}|} I_{lk}(\boldsymbol{x}, t) \ , \tag{1}$$

$$\left(\frac{\partial}{\partial t} + \gamma_{lk}\right)\left(\frac{\partial}{\partial t} + \tilde{\gamma}_{lk}\right) I_{lk}(\boldsymbol{x}, t) = \Gamma_{lk} e^{\gamma_{lk}\delta_{lk}} \cdot \tilde{\gamma}_{lk}\left[N_{lk}^{\beta} S_l(h_l) + \Phi_{lk}(\boldsymbol{x}, t) + p_{lk}(\boldsymbol{x}, t)\right] \ , \tag{2}$$

$$\tilde{\gamma}_{lk}/\gamma_{lk} = e^{\varepsilon_{lk}} \ , \qquad \tilde{\gamma}_{lk} - \gamma_{lk} = \varepsilon_{lk}/\delta_{lk} \ , \tag{3}$$

$$S_k(h_k) = S_k^{\max} / \left\{1 + (1 - r_{\mathrm{abs}} S_k^{\max}) \cdot \exp\left[-\sqrt{2}\,\frac{h_k(\boldsymbol{x}, t+\xi) - \bar{\mu}_k}{\hat{\sigma}_k}\right]\right\} \ , \tag{4}$$

$$\left[\left(\frac{\partial}{\partial t} + v\Lambda_{ek}\right)^2 - \frac{3}{2}v^2\nabla^2\right]\Phi_{ek}(\boldsymbol{x}, t) = v^2\Lambda_{ek}^2 N_{ek}^{\alpha} S_e(h_e) \ , \qquad \Phi_{ik}(\boldsymbol{x}, t) \equiv 0 \ . \tag{5}$$

Eq. (1) determines the mean soma membrane potential under weighted input from synaptic activity. The presynaptic sources summed in the square brackets of Eq. (2) are local, cortico-cortical, and extra-cortical, respectively. For a single presynaptic spike (Dirac delta at $t = 0$) the postsynaptic potential (PSP) response from Eq. (2) is bi-exponential. Suppressing subscripts for simplicity one finds: $I(t > 0) = \Gamma e^{\gamma\delta}\tilde{\gamma}\left(e^{-\gamma t} - e^{-\tilde{\gamma} t}\right)/\left(\tilde{\gamma} - \gamma\right)$. This models "fast" excitatory (AMPA / kainate) and inhibitory ($\mathrm{GABA_A}$) neurotransmitter kinetics. Maximum PSP amplitude Γ is reached at rise time δ: $I(t = \delta) = \Gamma$, whereas ε controls the decay time: $\zeta \simeq [0.9\varepsilon + 2\sinh\varepsilon + 0.3\tanh(0.8\varepsilon)]\delta/\varepsilon$ with $I(t = \zeta) = \Gamma/e$. For $\varepsilon \to 0 : \tilde{\gamma} \to \gamma$, see Eq. (3). The $\varepsilon = 0$ limit used in earlier works [11] yields the "alpha form" PSP response $I(t > 0) = \Gamma\gamma t e^{1-\gamma t}$, which couples rise and decay times $\zeta = 3.14\delta$. This is too restrictive for some applications [9].

Local mean firing rates are given by Eq. (4). Finally, long range excitation spreads according to Eq. (5). The numerical solution, eigensystem-based approximation, and parameter selection used here follow Ref. [9]. We work with the parameter set of Table 1 in the following. It was found in Ref. [9] in a search for physiological firing rates, reasonable power spectrum, and a "bi-phasic" power surge response to GAs. Other parameter sets with quite different but also physiological parameter values show similar behaviour.

Differential increases in $\Gamma_{ie,ii}$ have been shown to reproduce a shift from alpha to higher frequency beta band EEG activity (the "beta buzz") in the presence of low levels of $\mathrm{GABA_A}$-agonists such as the benzodiazepines [12]. Furthermore, the dynamics of linearized solutions of our model are particularly sensitive to variations in the parameters affecting inhibitory neurotransmission [11], like N_{ii}^{β}. This suggest that stronger variations of these parameters could lead to the emergence of coherent, spatially structured oscillations at even higher gamma frequencies. But can this be achieved with variations in a reasonable physiological range? Here we show that minor reductions in the mean inhibitory PSP (IPSP) amplitudes, $\Gamma_{ie,ii}$, and an even smaller increase in the mean local inhibitory-inhibitory connectivity, N_{ii}^{β}, are both sufficient to induce a spatially ordered 40 Hz state.

resting	h_e^{r}	-72.293 mV		h_{ee}^{eq}	7.2583 mV
potential	h_i^{r}	-67.261 mV	Nernst	h_{ei}^{eq}	9.8357 mV
decay	τ_e	32.209 ms	potential	h_{ie}^{eq}	-80.697 mV
time	τ_i	92.260 ms		h_{ii}^{eq}	-76.674 mV
	Γ_{ee}	0.29835 mV		γ_{ee}	122.68/s
PSP amp.	Γ_{ei}	1.1465 mV	PSP rate	γ_{ei}	982.51/s
	Γ_{ie}	1.2615 mV		γ_{ie}	293.10/s
	Γ_{ii}	0.20143 mV		γ_{ii}	111.40/s
	N_{ee}^{β}	4202.4	cort.-cort.	N_{ee}^{α}	3228.0
intra-cort.	N_{ei}^{β}	3602.9	#connect.	N_{ei}^{α}	2956.9
#connect.	N_{ie}^{β}	443.71	c.-c. decay	Λ_e	0.60890/cm
	N_{ii}^{β}	386.43	& cond. vel.	v	116.12 cm/s
maximum	$S_e^{\max}$	66.433/s		p_{ee}	2250.6/s
firing rate	$S_i^{\max}$	393.29/s	extra-cort.	p_{ei}	4363.4/s
firing	$\bar{\mu}_e$	-44.522 mV	input	p_{ie}^*	0/s
thresholds	$\bar{\mu}_i$	-43.086 mV		p_{ii}^*	0/s
std. dev.	$\hat{\sigma}_e$	4.7068 mV	syn. delay	ξ^*	0 ms
thresholds	$\hat{\sigma}_i$	2.9644 mV	abs. refract.	r_{abs}^*	0 ms

Table 1
The 37 parameter values used in this paper for Eqs. (1)-(5). Parameters marked with a star remained fixed and $\Lambda_e = \Lambda_{ee} = \Lambda_{ei}$ in searching a baseline solution, see Ref. [9]. Other physiologically valid parameter sets show similar behaviour.

2. Results

Fig. 1-*Left* shows a bifurcation diagram calculated with `XPPAUT` [13] for changes of the inhibitory PSP (IPSP) amplitudes $\Gamma_{ie,ii} \to r\Gamma_{ie,ii}$. Upon reducing the IPSP amplitude the system moves from a stable fixed point (solid line) to an unstable one (dot-

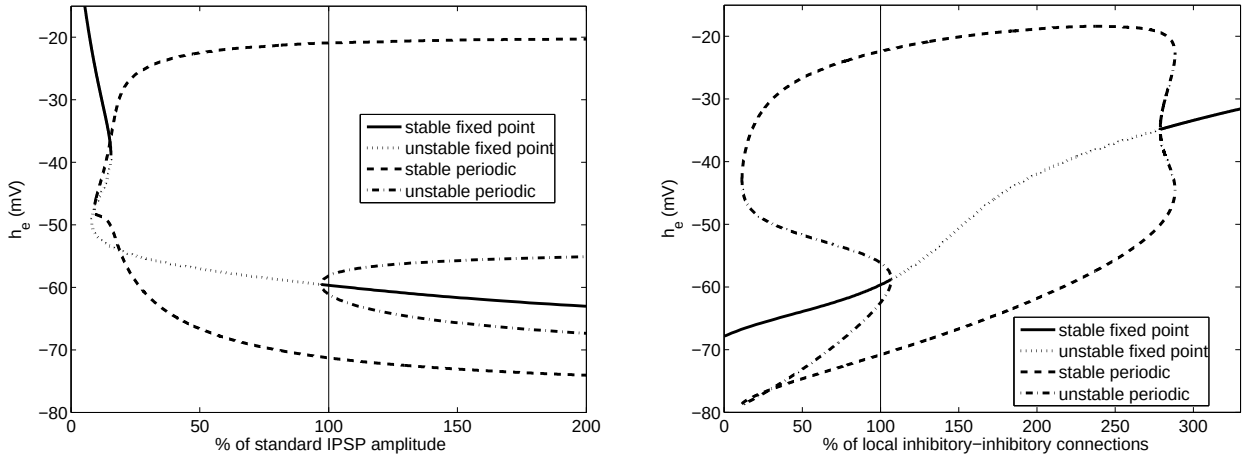

Fig. 1. Lines labeled "periodic" indicate extremal oscillation amplitudes. *Left*: Bifurcation diagram for changes of the IPSP amplitudes $\Gamma_{ie,ii} \to r\Gamma_{ie,ii}$, with r in %. *Right*: Similarly for local inhibitory-inhibitory connectivity $N_{ii}^{\beta} \to rN_{ii}^{\beta}$.

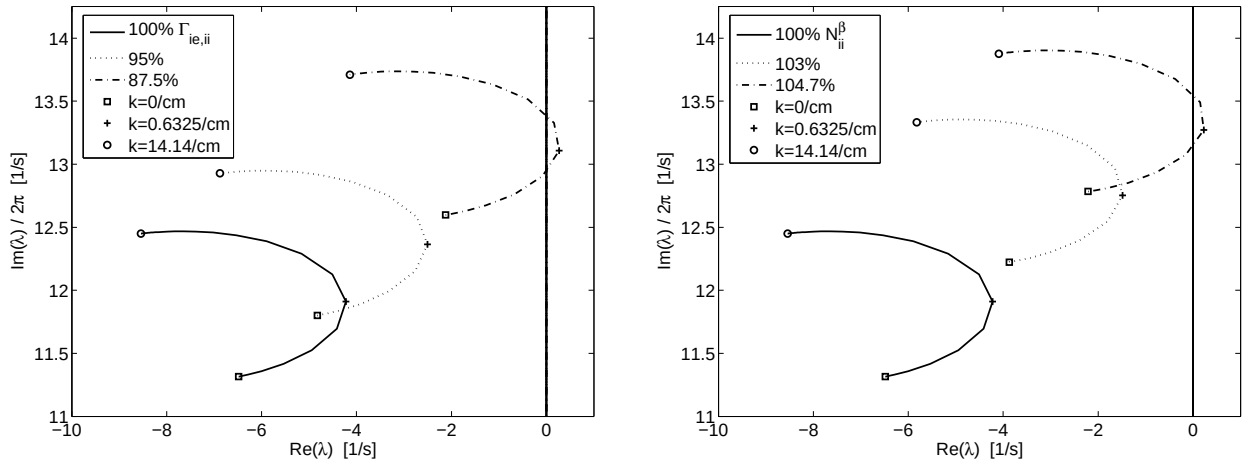

Fig. 2. *Left*: Motion of least damped eigenvalue $\lambda(k)$ by reducing IPSP amplitudes by 12.5%. The range of spatial wavenumbers k corresponds to physiological extra-cortical input. *Right*: Similarly by raising local inhibitory-inhibitory connectivity by 4.7%.

ted line), and a phase transition to stable periodic oscillations (between the dashed lines) occurs. The frequency of this limit cycle is in the gamma range (about 37 Hz). It is possible to induce these oscillations at full IPSP amplitude, if the EEG variable h_e is externally perturbed past the basin boundary of unstable periodic oscillations (dash-dotted lines). But lowering the IPSP amplitude will instead lead to a spontaneous emergence via a subcritical Hopf bifurcation.

We track the least damped eigenvalue $\lambda(k)$ of the linearized model in Fig. 2-*Left*. It dominates the frequency content of the power spectrum. The range of spatial wavenumbers k shown here is appropriate for physiological extra-cortical input [9]. For $r = 87.5\%$, the eigenvalue becomes unstable ($\mathrm{Re}[\lambda(k)] > 0$) at some wavenumbers. This corresponds to moving from the stable to the unstable fixed point in the bifurcation diagram. Since the eigenvalue becomes unstable only at a restricted range of wavenumbers, whereas most remain stable, we call this a marginal instability.

Fig. 3-*Left* shows the predicted corresponding change in power spectra. The original (100%) spectrum shows the features we expect for a human EEG at rest. The shift of the spectrum to higher frequencies upon reducing the IPSP amplitude is readily apparent. The linearized prediction of the spectrum at 87.5% is necessarily flawed, since it requires stable eigenvalues. Also at 87.5% IPSP amplitude a full simulation was run for a human-sized toroidal cortical sheet and a clear transition in

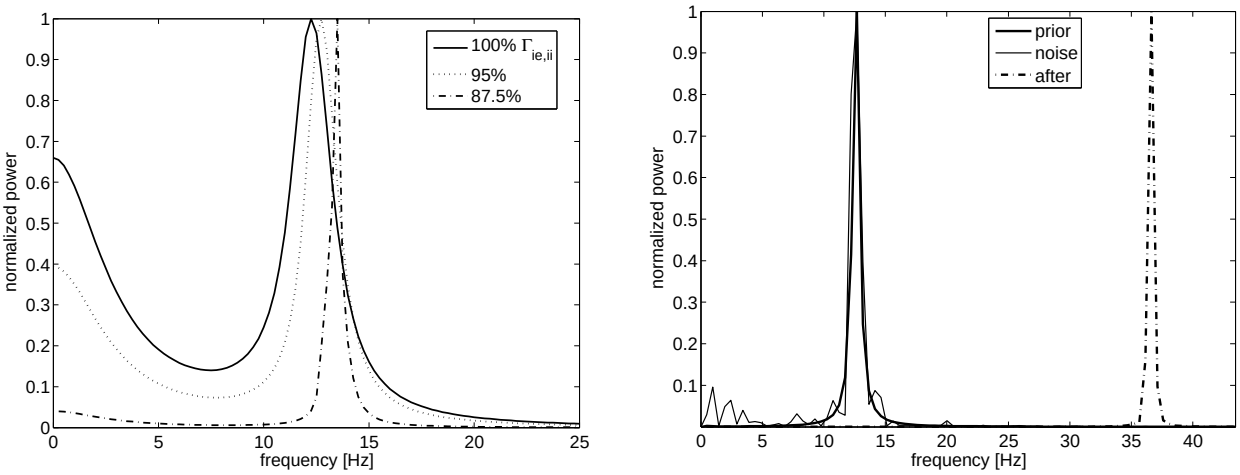

Fig. 3. Power spectra are normalized to their peak power. *Left*: Predictions for IPSP amplitudes at 100%, 95%, and 87.5% of values in Tab. 1. *Right*: Simulation results before and after transition in Fig. 4 with 87.5% IPSP amplitudes and random h_e initial conditions. The prior spectrum with noise (thin solid line) matches the prediction in spite of $\exists k:\ \mathrm{Re}[\lambda(k)] > 0$.

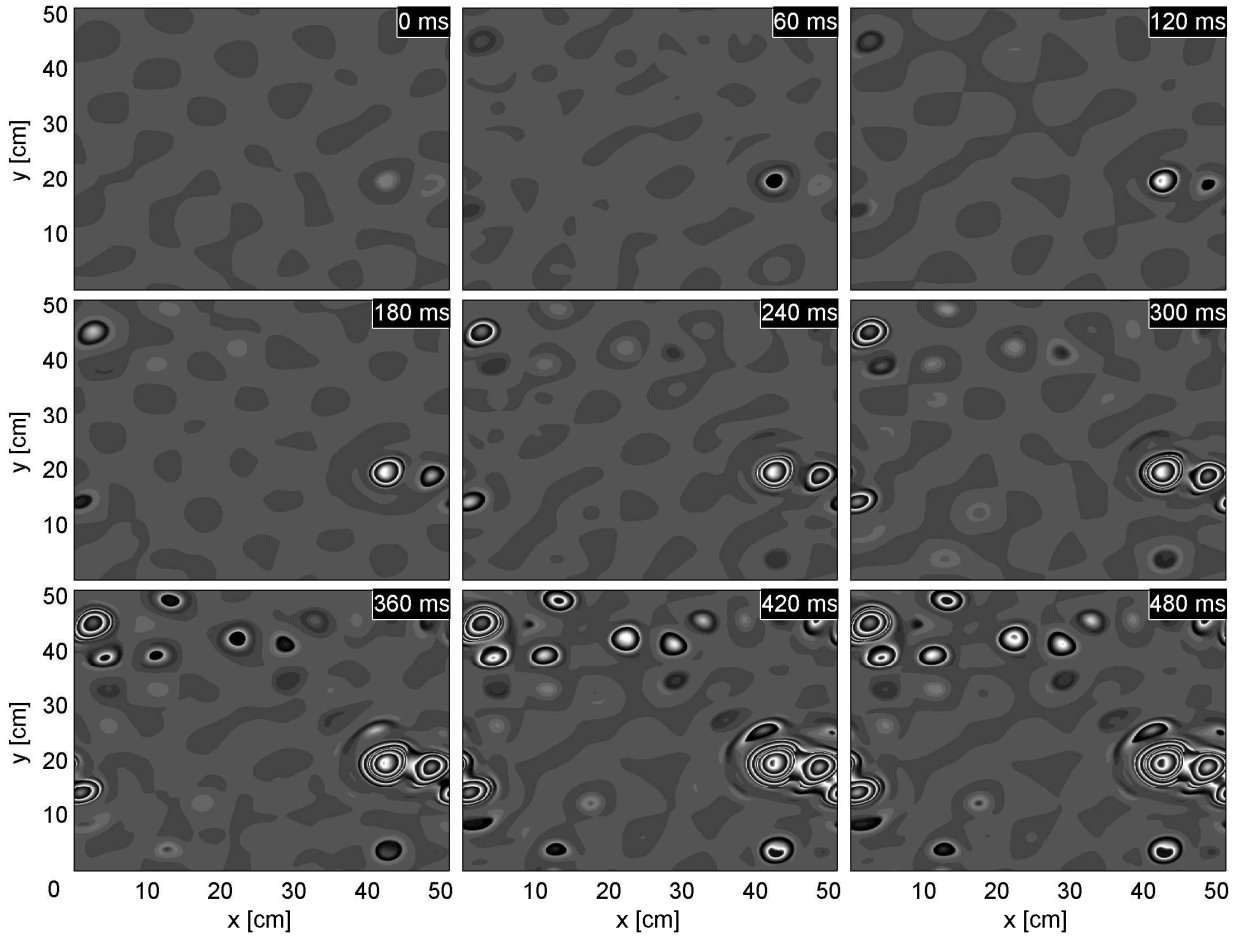

Fig. 4. Emergence of synchronized gamma activity, h_e mapped every 60 ms (-76.9 mV, black to -21.2 mV, white).

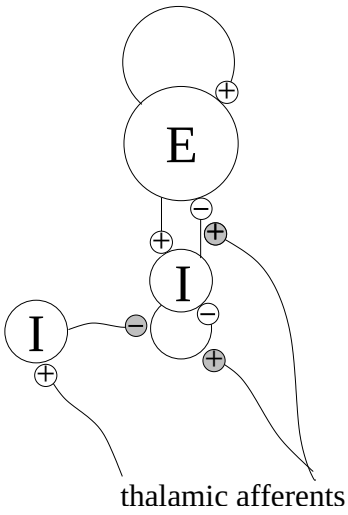

Fig. 5. Mechanisms by which thalamic afferents may alter inhibitory connectivity. (+) and (-) denote excitatory and inhibitory synaptic connections, respectively. Shaded connections are presynaptic (axo-axonic) rather than synaptic (axo-dendritic), with paradoxical effects on the target axon, e.g., a shaded (-) *facilitates* GABA release at the target axon's terminal. Thalamic afferents may excite inhibitory interneurons in layer IV, which then presynaptically facilitate GABA release on inhibitory neurons (left). Alternatively, they may presynaptically inhibit GABA release on both excitatory and inhibitory neurons (right).

frequency with the appearance of spatial patterns was observed. Fig. 3-*Right* shows how the average power spectrum, calculated before (solid line) and after (dash-dotted line) the transition, undergoes a dramatic shift to gamma frequencies.

The simulation was started from random initial conditions in h_e, but without extra-cortical noise input. This made it easier to observe clear emerging patterns. If one provides extra-cortical noise input a similar transition occurs. It is interesting that with noise the power spectrum prior to the transition (thin solid line) is remarkably similar to the in principle flawed prediction from the linearized model. The observed frequency transition is consistent with the predicted subcritical Hopf bifurcation. However, which features of the model and which parameter combinations establish the potential for such transitions in the first place is currently unknown and requires further research.

Fig. 4 shows part of the transition at 60 ms intervals by maps of electrocortical activity (grayscale shows $h_e = -76.9$ mV, black to -21.2 mV, white). In the first frame a focus of gamma activity begins to emerge (middle right). 120-180 ms later a second focus emerges (top left) at about 25 cm distance. Possibly a scalp electrode would only pick up stronger activity, e.g., the activity around the same locations at 240-300 ms and 360-420 ms, respectively. Further gamma "hot spots" continue to emerge throughout. The visible phase correlations between different foci have been confirmed by calculating instantaneous Hilbert phases.

If we choose to vary instead of $\Gamma_{ie,ii}$ the inhibitory-inhibitory connectivity in the local macrocolumn N_{ii}^{β}, we obtain the bifurcation diagram shown in Fig. 1-*Right*. This time we can cause the phase transition to a gamma frequency limit cycle by raising the parameter value till a subcritical Hopf bifurcation occurs. Fig. 2-*Right* confirms this for the least damped eigenvalue. Remarkably, the change induced by varying N_{ii}^{β} is very similar to varying $\Gamma_{ie,ii}$, although we only need to raise N_{ii}^{β} by 4.7% to achieve marginal instability. It should be understood that in general changes in different parameters can have wildly different effects. The predicted power spectra and indeed the numerical simulation of cortex produce very similar results to those already shown for $\Gamma_{ie,ii}$ and are not shown here.

3. Conclusions

Our theoretical analysis to date suggests that cortex may be conceived as being in a state of marginal linear stability (with alpha activity) and that this linear stability can be lost, by a range of perturbations, and replaced by a rapidly emerging ($\sim$ 150 ms) spatially synchronized 40 Hz state. This spatially structured state may be the physiological correlate of the perceptual act. On the basis of a previous analysis of parametric sensitivity [11], we investigated two broad types of parametric perturbation that were able to effect such a transition. The first involved the simultaneous reduction in the mean IPSP amplitudes, whereas the second involved an increase in the strength of local inhibitory-inhibitory connectivity.

What, if any, physiological mechanism could account for such modifications? One possibility presenting itself is that of presynaptic inhibition or presynaptic facilitation. It is a surprising fact that thalamic afferents contribute only some 5-10% of all axon terminals in cortex [14]. Further, even though the termination of thalamic afferents is restricted principally to layer IV, they lack specificity in the sense that they do not show any preference for their postsynaptic target. Thus a variety of neuron types

(excitatory and inhibitory) in layer IV receive thalamic afferents. Because the fraction of inhibitory synapses in cortex ($\approx 15\%$, see for example Ref. [15]) is about the same order as the number of thalamic terminals it is possible that excitatory thalamic afferents might reduce effective IPSP amplitudes through the inhibition of presynaptic GABA release. We have modelled this effect here by reducing $\Gamma_{ie,ii}$.

Alternatively, excitatory thalamic afferents may excite a range of layer IV interneurons which presynaptically facilitate inhibitory-inhibitory connectivity, i.e., enhance the presynaptic release of GABA. Both mechanisms are illustrated in Fig. 5. The second of these mechanisms seems the more plausible as hippocampal interneurons have been shown to enhance the presynaptic release of GABA [16]. This effect has been modelled here by raising N_{ii}^{β}. We have demonstrated that correlated gamma band activity indicative of large scale integration can emerge spontaneously for both cases in our physiological theory of EEG. The changes themselves were realistically small, particularly so for the more plausible mechanism modelled with N_{ii}^{β}.

Our work hence suggests that dynamic computation indicated by synchronous large-scale gamma activity can occur when minor brain state changes, possibly induced by the thalamus, lead to a marginal instability in cortex.

References

[1] F. Varela, J.-P. Lachaux, E. Rodriguez, J. Martinerie, The brainweb: Phase synchronization and large-scale integration, Nature Reviews Neuroscience 2 (2001) 229–239.

[2] R.D. Traub, J.G.R. Jefferys, M.A. Whittington, Fast Oscillations in Cortical Circuits, MIT Press, Cambridge, MA, 1999.

[3] E. Rodriguez, N. George, J.-P. Lachaux, J. Martinerie, B. Renault, F.J. Varela, Perception's shadow: long distance synchronisation of human brain activity, Nature 397 (1999) 430–433.

[4] C. Tallon-Baudry, O. Bertrand, C. Delpuech, J. Pernier, Oscillatory γ-band (30-70 hz) activity induced by a visual search task in humans, Journal of Neuroscience 17 (1997) 722–734.

[5] S.L. Bressler, R. Coppola, R. Nakamura, Episodic multiregional cortical coherence at multiple frequencies during visual task performance, Nature 366 (1993) 153–156.

[6] A.K. Engel, P. Fries, W. Singer, Dynamic predictions: Oscillations and synchrony in top-down processing, Nature Reviews Neuroscience 2 (2001) 704–716.

[7] W. Singer, C.M. Gray, Visual feature integration and the temporal correlation hypothesis, Annual Reviews of Neuroscience 18 (1995) 555–586.

[8] C. von der Malsberg, W. Schneider, A neural cocktail party processor, Biological Cybernetics 54 (1986) 29–40.

[9] I. Bojak, D.T.J. Liley, Modeling the effects of anesthesia on the electroencephalogram, Physical Review E71 (2005) 041902, 1–21.

[10] D.T.J. Liley, I. Bojak, Understanding the transition to seizure by modelling the epileptiform activity of general anaesthetic agents, Journal of Clinical Neurophysiology 22 (2005) 300–313.

[11] D.T.J. Liley, P.J. Cadusch, M.P. Dafilis, A spatially continuous mean field theory of electrocortical activity, Network: Computation in Neural Systems 13 (2002) 67–113.

[12] D.T.J. Liley, P.J. Cadusch, M. Gray, P.J. Nathan, Drug-induced modification of the system properties associated with spontaneous human electroencephalographic activity, Physical Review E68 (2003) 051096, 1–15.

[13] B. Ermentrout, Simulating, Analyzing, and Animating Dynamical Systems, Society for Industrial and Applied Mathematics, Philadelphia, 2002.

[14] A. Peters, Examining neocortical circuits: Some background and facts, Journal of Neurocytology 31 (2002) 183–193.

[15] V. Braitenberg, A. Schüz, Anatomy of the Cortex: Statistics and Geometry, 2nd Edition, Springer Verlag, Berlin, 1998.

[16] D. Cuhna-Reis, A.M. Sebastio, K. Wirkner, P. Illes, J.A. Ribeiro, VIP enhances both pre- and postsynaptic GABAergic transmission to hippocampal interneurones leading to increased excitatory synaptic transmission to ca1 pyramidal cells, British Journal of Pharmacology 143 (2004) 733–744.